Silicon Carbide Merged PiN Schottky Diode Switching Characteristics and Evaluation for Power Supply Applications

A. Hefner, Jr. and D. Berning
Semiconductor Electronics Division
National Institute of Standards and Technology
Gaithersburg, MD 20899

J. S. Lai and C. Liu
Virginia Polytechnic Institute and State University
Center for Power Electronics Systems
Blacksburg, VA 24061-0111

R. Singh
Cree Inc.
4600 Silicon Drive
Durham, NC 27703

***Abstract*–A newly developed Silicon Carbide (SiC) Merged PiN Schottky (MPS) diode combines the best features of both Schottky and PiN diodes to obtain low on-state voltage drop, low leakage in the off-state, fast switching, and good high temperature characteristics. In this paper, the switching characteristics of 1500-V, 0.5-A rated SiC MPS diodes are evaluated and compared to the fastest, similarly rated silicon diodes available. Experimental results indicate that the reverse recovery time and associated losses are nearly zero for the SiC MPS diodes. By replacing the best silicon diodes available with a SiC MPS diode, the efficiency of a test-case power supply was found to increase from 89 % to 91.5 % for switching at 100 kHz, and from 82 % to 88 % at 186 kHz. A significant electro-magnetic interference (EMI) reduction was also obtained with the SiC MPS diodes compared to the silicon diodes for the noise spectrum range from 70 MHz to 150 MHz.**

I. INTRODUCTION

Silicon Carbide (SiC) power devices are expected to show superior performance compared to devices made with other semiconductors. This is primarily because 4H-SiC has an order of magnitude higher breakdown electric field (2-4×10^6 V/cm) and higher temperature capability than conventional silicon (Si) materials. The high breakdown electric field allows the design of SiC power devices with thinner and more highly doped voltage blocking layers. A comparison of the ideal breakdown voltage versus blocking layer doping concentration is shown in Fig. 1. The more highly doped blocking layer (more than 10 times higher) provides lower resistance for SiC devices because more majority carriers are present than for comparably rated silicon devices. A comparison of the voltage blocking layer thickness for a given breakdown voltage is shown in Fig. 2. The thinner blocking layer of SiC devices ($1/10^{th}$ that of silicon devices) also contributes to the lowering of the specific on-resistance by a factor of 10. The combination of $1/10^{th}$ the blocking layer thickness with 10 times the doping concentration can yield a SiC device with a factor of 100 advantage in resistance compared to that of Si devices.

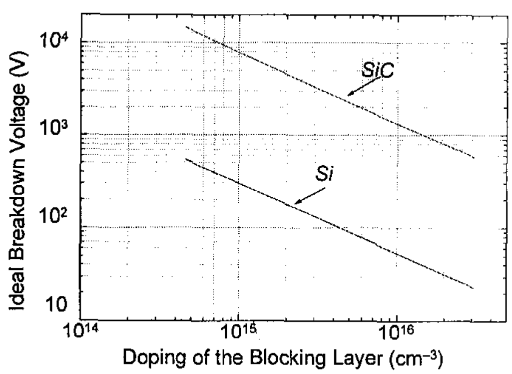

Fig.1. Comparison of the ideal breakdown voltage of Si and SiC devices for different doping levels.

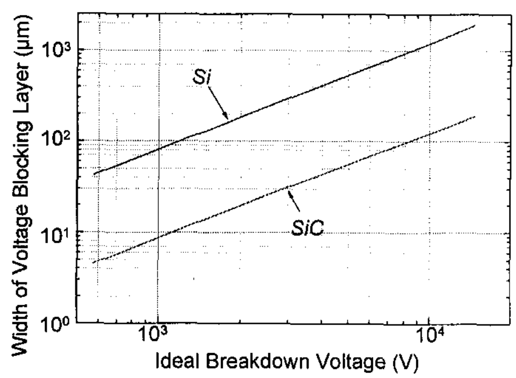

Fig.2. Comparison of the blocking layer thickness as a function of the ideal breakdown voltage for SiC and Si.

Because SiC has a larger band gap (3.26 eV for 4H-SiC [1] vs. 1.1 eV for Si), SiC devices can be made to operate reliably at much higher temperatures than their silicon counterparts (300 °C for SiC vs. 150 °C for Si).

Recently, SiC Merged PiN Schottky (MPS) diodes have been developed that combine the advantages of both Schottky and PiN diodes [2,3]. These diodes show great potential for switching power supply applications. The main features of this SiC MPS diode are (1) low voltage drop in the on-state

† Contribution of the National Institute of Standards and Technology is not subject to copyright. This work was partially supported by the DARPA Megawatt Solid-State Elec. Program, and made use of ERC Shared Facilities supported by the National Science Foundation award EEC-9731677.

0-7803-6401-5/00/$10.00 © 2000 IEEE

like the Schottky, (2) low leakage in the off-state like the PiN, (3) fast switching characteristics like the Schottky, and (4) good high temperature characteristics. In this paper, several circuits and methods for evaluating the switching characteristics of ultra fast Si and SiC diodes are presented. The newly designed 1500-V, 0.5-A rated SiC MPS diodes are evaluated and compared to the fastest silicon diodes.

It is shown in this paper that the reverse recovery of the SiC MPS diode is primarily capacitive in nature and that the stored charge is nearly zero. Because the reverse recovery is capacitive for the SiC MPS diodes, the voltage rises at the beginning of the reverse recovery period as opposed to silicon devices, where the voltage rise is delayed by the stored charge recovery. This results in a dramatic reduction in the turn-on loss for the anti-parallel switching device (e.g., IGBT, MOSFET, or CoolMOS‡) in high frequency switching power supplies and adjustable speed drives. By replacing the fastest silicon diodes available with a SiC MPS diode, the measured power supply efficiency is found to increase from 89 % to 91.5 % for switching at 100 kHz, and from 82 % to 88 % at 186 kHz in a test case. Significant electromagnetic interference (EMI) reduction over the silicon diode is found between 70 MHz and 150 MHz.

II. SiC Merged PIN Schottky Diode

Generally speaking, there are three classes of SiC power rectifiers: (a) Schottky diodes, which offer extremely high switching speed but suffer from high leakage current; (b) PiN diodes, which offer low leakage current but show reverse recovery charge during switching and have a large junction voltage drop due to the wide band gap of 4H-SiC; and (c) Merged PiN Schottky (MPS) diodes, which offer Schottky-like on-state and switching characteristics, and PiN-like off-state characteristics.

A cross-section of a 4H-SiC MPS rectifier operating in the forward-bias (left) and reverse-bias (right) condition is shown in Fig. 3. An MPS diode consists of interdigitated Schottky and p^+-implanted areas. For on-state drops of <3 V, only the Schottky regions of the diode conduct and thus the device is also referred to as a Junction Barrier Schottky (JBS) diode. The on-state voltage drop of the MPS diode is determined by (1) the resistance of the drift region, (2) the metal-SiC barrier height of the Schottky metal, and (3) the relative area of the Schottky vs. the p^+ implanted regions.

For reverse bias conditions, the depletion regions from adjacent p^+ implanted regions pinch-off the leakage current arising from the Schottky contacts of the device. The leakage current in the Schottky regions occurs due to Schottky barrier lowering at the metal-n^- junction. The presence of the adjacent p^+-implanted regions reduces the electric field at the metal-SiC junction because of two-dimensional charge sharing. This property is especially useful when the diode is operating at elevated temperatures since the effect of Schottky barrier lowering is enhanced with increasing temperature.

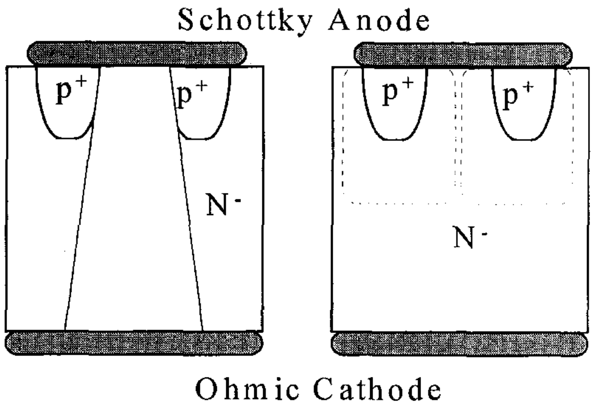

Fig. 3. MPS diode forward on-state current flows through the Schottky Anode (left), while reverse leakage current is limited by depletion from adjacent p^+ grids (right).

The detailed design of the 1500-V MPS diodes are described in ref. [3]. The design primarily consists of selecting the optimal Schottky metal, size and spacing of the p^+-implanted regions, and thickness and dopant density of the drift region. It is important to achieve a good quality Schottky interface to obtain a low on-state drop when operated in the JBS diode mode. The metal-SiC barrier height of the Schottky metal should be low enough to give a low on-state voltage, while still enabling effective pinch-off during the off state. This is achieved using Ni as the Schottky metal.

The rectifiers were made using a 20-μm, N_D=2E15-cm^{-3} epitaxial layer over 4H-SiC n^+ substrates to obtain the desired blocking voltage of 2000 V. In this first lot of samples described in this paper, the actual blocking capability was 1500 V. However, the blocking voltage is expected to increase to near 2000 V with further process refinements. There exists a fundamental trade-off between the on-state voltage and leakage current of the MPS diode. The design parameters that affect this trade off are (1) the relative area of the p^+ implanted region, and (2) the geometrical layout of the p^+ implanted region. A large p^+ implanted area is expected to result in a higher on-state voltage due to a smaller Schottky conducting area, but may offer lower leakage due to a more effective pinch-off of the Schottky portion.

The optimized diodes produced in [3] have a 2-μm wide p^+ implanted region with 4-μm spacing. The two geometric p^+ layouts implemented on the mask design are the linear p^+ grid and the honeycombed p^+ grid. While the honeycombed design offers a more effective pinch-off of the leakage current, a larger area is not conducting for a given distance between adjacent Schottky regions. In order to optimize the design of the MPS diodes, four kinds of devices were

‡ Cool MOS™ is a trademark of Infineon Technologies, Germany. Certain commercial products or materials have been identified in order to specify or describe the subject matter of this paper adequately. This does not imply recommendation or endorsement by the National Institute of Standards and Technology, nor does it imply that the products are the best for the purpose.

designed on the same mask: honeycomb grid MPS diodes, linear grid MPS diodes, implanted PiN diodes, and Schottky diodes. Several device areas giving current ratings from 0.5 A to 4 A were produced, although the results shown in this paper are for the 0.0045 cm^2 samples having a 0.5 A current rating.

III. STATIC CHARACTERISTICS

To determine the effectiveness of the MPS diode concept, it is important to compare the on-state voltage and reverse bias I-V characteristics of Schottky diodes, MPS diodes, and PiN diodes fabricated on the same wafer. Fig. 4 shows the comparison of on-state J-V characteristics of such Schottky, linear MPS, honeycomb MPS, and PiN diodes. For a current density of 100 A/cm^2, an on-state voltage of 1.9 V was obtained for the linear MPS diodes operated in the JBS mode. The on-state characteristics of the Linear MPS and Schottky diodes are almost identical, indicating excellent current spreading and minimal increase in the on-state voltage due to the introduction of the p^+ implanted grid.

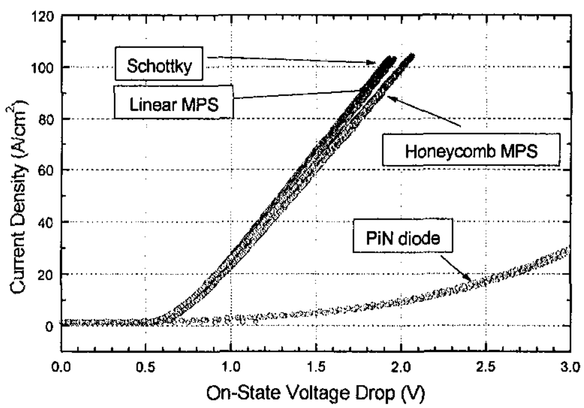

Fig. 4. Measured on-state J-V comparison for Schottky, linear MPS, honeycomb MPS, and PiN diodes fabricated on the same wafer.

The reverse bias characteristics of honeycomb MPS and linear MPS diodes are much more similar to the PiN diodes than to the Schottky diodes. At a leakage current density of 2 mA/cm^2, the blocking voltages of Schottky, honeycomb MPS, linear MPS, and PiN diodes are measured to be 610 V, 1380 V, 1480 V, and 1980 V, respectively. A blocking voltage of 1500 V is achieved for the Linear MPS diode at a leakage current density of 3 mA/cm^2, as shown in Fig. 5. This blocking voltage is achieved for the full range of device areas produced. The leakage current is negligible up to 1200 V.

The measured temperature dependence of the on-state characteristics for a 1500-V, 0.5-A (0.0045 cm^2) rated SiC MPS diode is shown in Fig. 6. The increase in on-state voltage with temperature is indicative of the reduction of mobility with temperature for a majority carrier device. Although this positive temperature coefficient of resistance increases the on-state loss at high temperature, it is beneficial for paralleling and large area current sharing. For comparison, Fig. 7 shows the measured temperature dependence of on-state voltage for a 1000-V, 1-A rated ultra-fast silicon PiN diode (MUR1100).

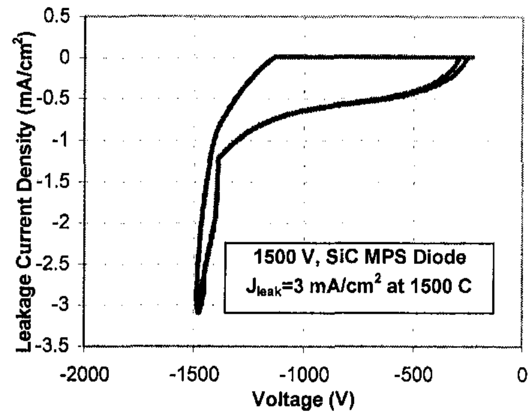

Fig. 5. Reverse bias characteristics of the linear MPS diode.

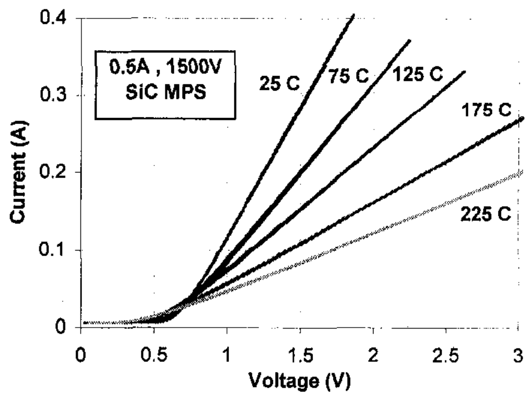

Fig. 6. Measured temperature dependence of the on-state characteristics for a 1500-V, 0.5-A (0.0045 cm^2) rated SiC MPS diode.

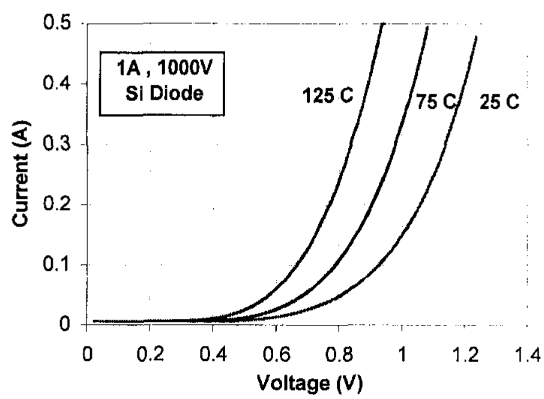

Fig. 7. Measured temperature dependence of on-state voltage for a 1000-V, 1-A rated ultra-fast silicon PiN diode (MUR1100).

IV. Switching Characteristics

Fig. 8 shows the test circuit used for characterizing the diodes for reverse recovery. A 5-cycle burst at a 100-Hz rate causes a progressive build-up of current through the inductor, and measurements are made during the last cycle of the burst. A 6LF6 vacuum tube is used as a switch in place of the usual MOSFET switch to achieve low parasitic capacitance at the anode of the DUT, and extremely fast switching speed. The resistor R isolates the DUT from the parasitic capacitance of the inductor, and also is used to quickly reset the inductor current to zero after each 5-cycle test burst so that the DUT is not heated. The dv/dt of the square-wave drive burst to the tube can be adjusted to achieve different di/dt values for the DUT. With a 700 V peak drive to the screen grid of the tube, the test circuit can test up to 9 A of combined forward and reverse DUT current, and the applied voltage to the DUT can be up to 2000 V.

For the tests described in this paper, a 500 V supply is used and tests are performed for various values of di/dt and dv/dt where dv/dt is controlled by placing various capacitors across the DUT. Varying the value of dv/dt makes it easier to identify the portion of the diode recovery due to charge storage and the portion due to device capacitance. Adding values of capacitance to the output of the tube emulates the conditions of using anti-parallel switching devices of different output capacitance in an application circuit. By independently controlling the supply voltage, di/dt, and dv/dt, the new test circuit enables testing the diode for the full range of conditions that occur for various application conditions.

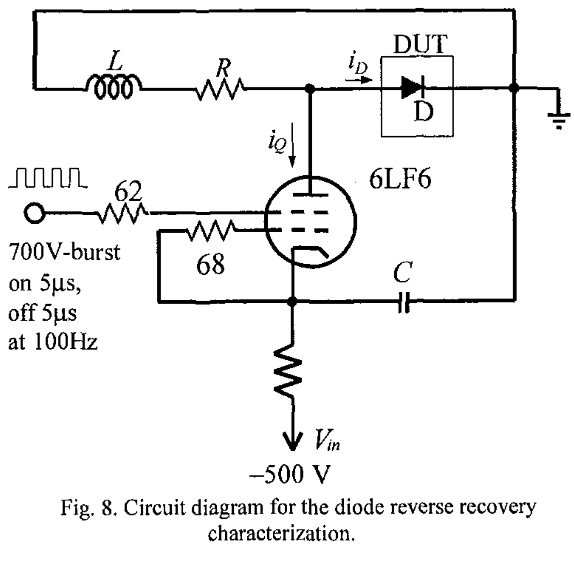

Fig. 8. Circuit diagram for the diode reverse recovery characterization.

Fig. 9 shows the measured turn-off characteristics of the MPS diode for three different di/dt values without an external driver capacitance. Fig. 10 shows the comparison of the turn-off characteristics with and without an external driver capacitance. These results show that even for the fastest turn-off, the recovery of the SiC diode is mostly capacitive in nature. This conclusion is reached by observing that the reverse voltage rise occurs during the entire reverse current period, and that the capacitive current is reduced with the added driver capacitance.

The internal diode capacitance can be readily calculated from these waveforms. For example, the middle turn-off speed curve in Fig. 9 (di/dt equal to 0.1 A/ns) has a maximum dv/dt equal to 60 V/ns and the maximum reverse current is 0.2 A at this point. Using these values, the capacitance is calculated to be 3.3 pF for this diode when the reverse voltage is equal to several hundred volts. This value is consistent with the junction depletion capacitance value calculated using the blocking region doping concentration.

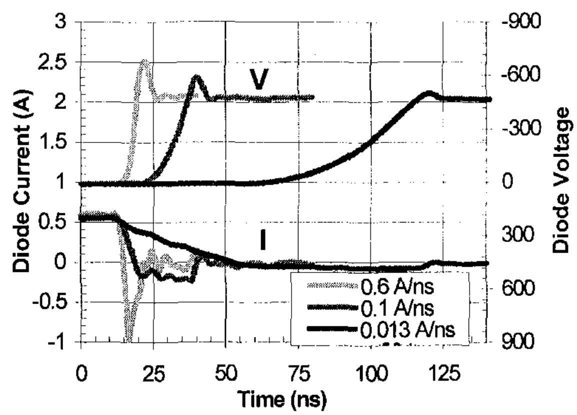

Fig. 9. SiC MPS diode reverse recovery characteristics at different di/dt values.

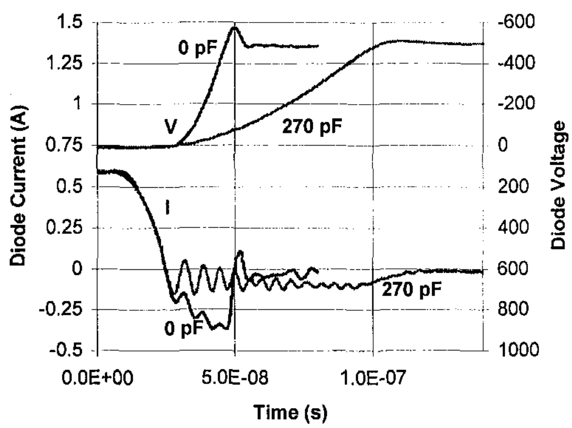

Fig. 10. SiC MPS diode reverse recovery characteristics with and without an added drive capacitance.

Fig. 11 shows a comparison between an ultra-fast 1000V silicon PiN diode and the SiC MPS diode. In contrast to the MPS diode, the bulk of the reverse recovery current in the silicon diode occurs before the voltage rises. This indicates that charge storage is far more important than junction capac-

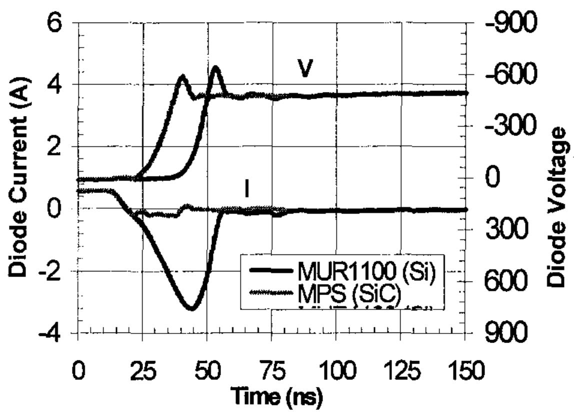

Fig. 11. Comparison of the reverse recovery characteristics of the SiC MPS and Si PiN diode MUR1100 at di/dt = 100A/µs.

itance in the Si diode. As can be seen in the figure, the voltage rise is delayed for the Si diode relative to the SiC MPS diode, even though the tube is turned on at the same time for both devices. The reverse-recovery current in the Si diode is huge in comparison to that of the SiC diode. Furthermore, the nature of the charge-storage-type recovery for the Si diode means that the anti-parallel switch (e.g., IGBT, MOSFET, or CoolMOS) in a hard-switched power converter experiences the full supply voltage at full current (load current plus diode current) during the switch turn-on. In contrast, the anti-parallel switch experiences less voltage during turn-on with the SiC MPS diode because the voltage begins to rise at the beginning of the diode recovery.

Figs. 12 and 13 show the temperature dependence of the reverse recovery waveform for the SiC MPS diode and the ultra-fast Si diode for the same di/dt value of 50 A/µs and a forward current of 0.6 A. Because the SiC MPS diode switching is dominated by junction capacitance, there is virtually no temperature dependence of the reverse recovery waveform over the range of 25 °C through 225 °C. The capacitance results in a peak reverse current of 0.4 A and a recovery time of 20 ns. For the ultra-fast Si diode, the peak reverse recovery current increases from 1.5 A to 2.7 A and the recovery time increases from 50 ns to 100 ns as the temperature is increased from 25 °C to 125 °C. This occurs because the lifetime increases with temperature. As a result, the Si diode recovery charge increases by approximately a factor of four over the 100 °C temperature range.

V. Power Supply Performance Evaluation

The power supply circuit shown in Fig. 14 can be used for step-up or step-down applications [4]. When switch Q turns on, inductors L_1 and L_2 are charged with current rise rates of $di_1/dt = V_{in}/L_1$, and $di_2/dt = V_{C1}/L_2$. When Q turns off, the diode D (DUT) conducts, and inductors L_1 and L_2 are discharged with current fall rates of $di_1/dt = (V_{in} - V_{C1} - V_o)/L_1$ and $di_2/dt = -V_o/L_2$.

Fig. 15 shows the idealized voltage waveform for switch Q, and also the current waveforms for inductor L_1, switch Q, and the DUT. Under steady-state continuous conducting conditions, the output voltage transfer ratio is $V_o/V_{in} = D/D'$, where D is the switch duty cycle, and $D' = 1 - D$. For step-down applications, D' is larger than 0.5, and the diode forward voltage drop is crucial for efficiency consideration. As the frequency of operation is increased, the diode reverse recovery becomes more important for the switch turn-on loss.

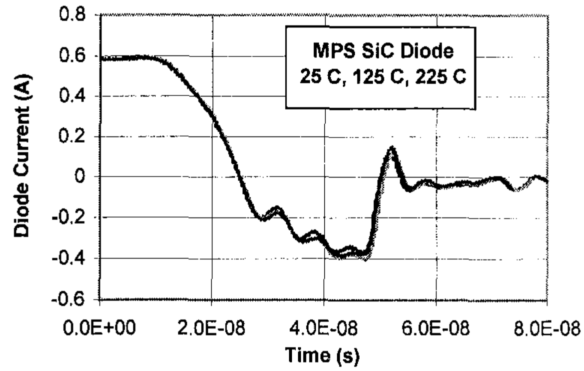

Fig. 12. Measured temperature dependence of the reverse recovery characteristics for a 1500-V, 0.5-A (0.0045 cm2) rated SiC MPS diode.

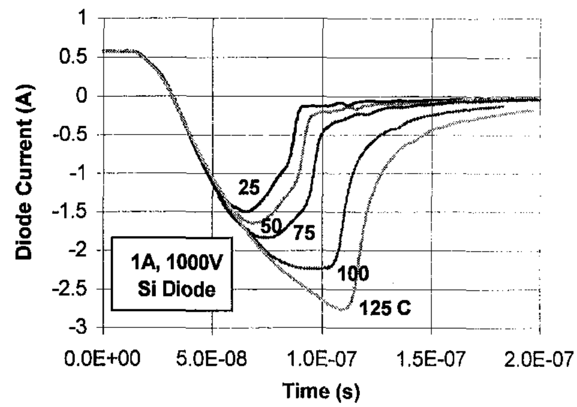

Fig. 13. Measured temperature dependence of the reverse recovery characteristics for a 1000-V, 1-A rated ultra-fast silicon PiN diode (MUR1100).

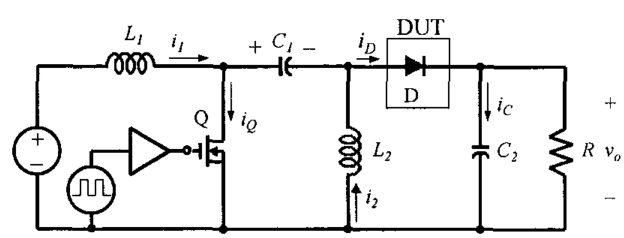

Fig. 14. Circuit diagram of a dc-dc converter for efficiency evaluation.

A. Experimental Setup

A 50 W power supply circuit was designed for a 500 V to 100 V step-down application. This test circuit uses a Cool MOS™ transistor for the switch [5,6]. With conventional ultra-fast reverse recovery diodes, the switching frequency is limited. In initial testing, several commercially available ultra-fast silicon diodes were destroyed at 100 kHz switching because of excessive diode reverse recovery losses. Because the 1000 V silicon diodes cannot operate under these conditions, the final comparison is made between the 1500 V SiC MPS diode and the 600 V silicon diode (BYV26C). The major circuit components used in this experiment are:

Q: SPP20N60S5 Cool MOSFET
D: BYV26C and SiC MPS test sample
L_1, L_2: 12 mH
C_1: 1 μF
C_2: 100 μF.

B. Switching Losses

With a fixed dc voltage, the turn-on and turn-off energies of switch Q, E_{on}, and E_{off}, can be considered as a function of the device current, i_Q. Because the switch turn-on current contains the diode reverse recovery current before the switch voltage drops to its on-state value, the turn-on energy loss is highly dependent on the diode (DUT) characteristics. The total device switching loss can be expressed as $P_{Q\text{-}sw} = f_{sw}(E_{on} + E_{off})$. Once the switching device voltage reaches its on-state value, the diode current starts returning to zero, and the switching loss due to this part of the diode reverse recovery can be expressed as $P_{D\text{-}rr} = f_{sw} \cdot E_{D\text{-}rr}$, where $E_{D\text{-}rr}$ is the diode switching energy associated with the diode reverse recovery.

C. Conduction Loss

The average conduction power loss for a device can be determined by integrating the instantaneous power loss over one switching cycle. If the inductors are large enough, the current ripple approaches zero, and the conduction loss can be calculated using the average load current. The conduction loss of the MOSFET and diode can be expressed as $P_Q = DI^2R_{DS\text{-}on}$ and $P_D = D'I(V_F + IR_{AK})$, where $R_{DS\text{-}on}$ is the switch on-resistance, and $V_F + IR_{AK}$ is the diode voltage drop under current I condition.

D. Efficiency Evaluation Results

Fig. 16 compares the efficiency measurement results with both SiC and Si diodes at 100 kHz switching frequency. The experimental results indicate that the system efficiency with a SiC MPS diode is between 91 % and 92 % for most load conditions. By comparison, the system efficiency with the BYV26C silicon diode varies between 88.5 % and 89.5 % under the same load conditions. The tests shown in Fig. 17 were performed at 186 kHz, and the results indicate that the full-load efficiency is 88 % with the SiC diode compared to 82 % with the silicon diode, a 6 % efficiency improvement.

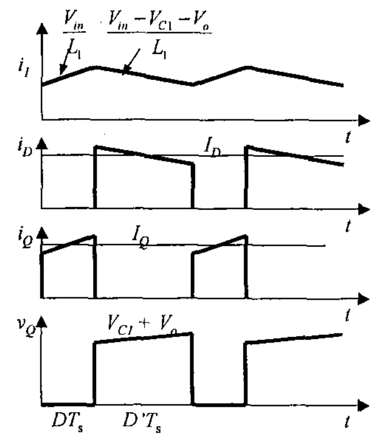

Fig. 15. Basic operating principle of the studied dc-dc converter.

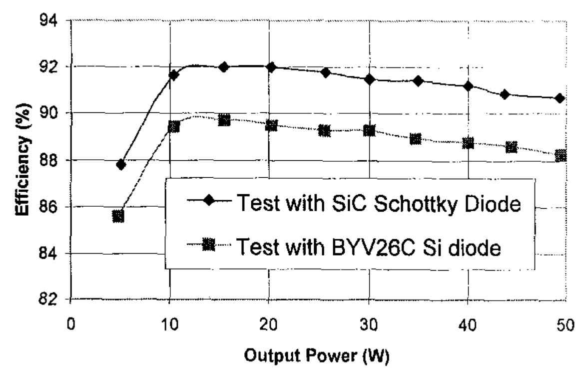

Fig. 16. Power supply efficiency comparison between the SiC MPS diode and an ultra-fast reverse recovery silicon diode at 100 kHz .

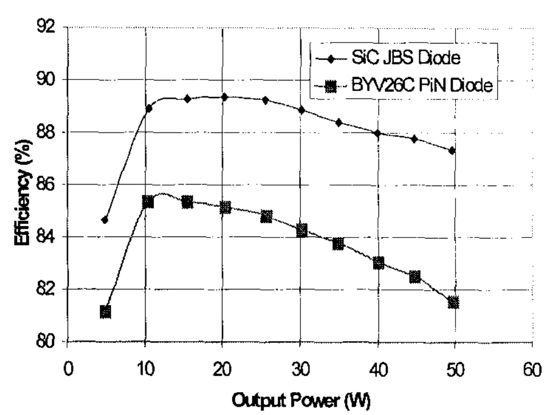

Fig. 17. Power supply efficiency comparison between the SiC MPS diode and an ultra-fast reverse recovery silicon diode at 186 kHz .

Fig. 18 compares the loss distribution between the systems with SiC and Si diodes at 100 kHz switching. The switching device and diode associated losses include five loss components: diode conduction (Dcon), switch conduction (Qcon), switch turn-on (SWon), switch turn-off (Swoff), and diode reverse recovery (Drr). The I^2R loss associated with the power supply inductor is included in the efficiency evaluation but not in the loss distribution comparison. With the Si diode, the most dominant loss component is the turn-on switching loss.

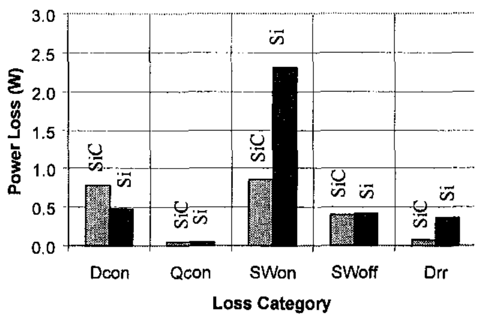

Fig. 18. Loss distribution at 100 kHz switching frequency for SiC MPS diode and an ultra fast reverse recovery silicon diode.

E. EMI Evaluation

The diode reverse recovery has been considered to be a major source of EMI [7]. With nearly zero reverse recovery time, the SiC diode is expected to emit less EMI high frequency noise components. Experiments were conducted to compare the EMI performance between the above mentioned Si and SiC diodes under the same converter conditions. Fig. 19 shows the experimental EMI spectrum for the frequency range from 30 MHz to 150 MHz. For comparison purposes, the EMI spectrum with Si diode is only shown with the envelope. The major EMI reduction with the SiC diode appears in the frequency range of 70 MHz to 150 MHz.

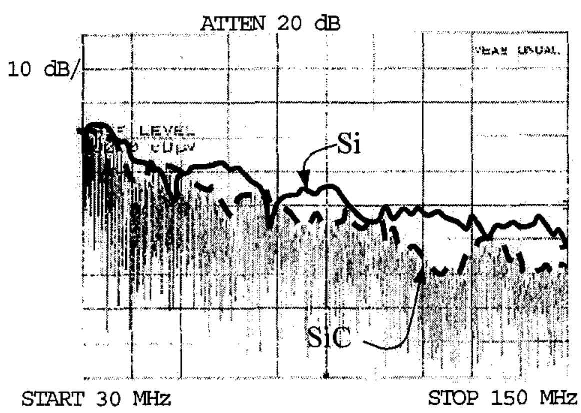

Fig. 19. Comparison of EMI spectrum envelope for the switching power supply with Si and SiC diodes.

VI. CONCLUSION

A newly designed silicon carbide Merged PiN Schottky diode combines the best features of both Schottky and PiN diodes, and exhibits low on-state voltage drop, low off-state leakage current, fast switching, and good high temperature characteristics. Several test circuits are presented for characterizing the reverse recovery and turn-on losses of high voltage, ultra fast silicon and wide-band-gap material diodes. The newly developed high-voltage silicon carbide diode demonstrates excellent features in reverse recovery improvement and switching loss reduction as compared to the traditional ultra fast silicon diodes, even those of lower voltage rating. The experimental results of 1500-V, 0.5-A rated MPS diodes indicate nearly zero reverse recovery time. The low reverse recovery charge also results in low turn-on losses for the anti-parallel switching device and reduced EMI high frequency components. By replacing the best silicon diodes available with a SiC MPS diode, the power supply efficiency was found to increase from 89 % to 91.5 % for switching at 100 kHz, and from 82 % to 88 % at 186 kHz.

ACKNOWLEDGMENT

The authors would like to thank Sébastien Bouché and Christophe Chapuy from University Montpellier II, France, and Telesphor Kamgaing from Motorola for laboratory instrumentation and data analysis.

REFERENCES

[1] N. G. Wright and D. J. Morrison, "Electrothermal Simulation of 4H-SiC Power Devices," *Materials Science Forum*, vol. 264-268, (1998).

[2] F. Dahlquist, J. O. Svedberg, C. M. Zetterling, M. Ostling, B. Breitholtz, and H. Lendenmann, "A 2.8 kV, 2V Forward Drop JBS Diodes with Low Leakage," *Proceedings of the International Conference of Silicon Carbide and Related Materials (ICSCRM)*, Oct. 1999.

[3] R. Singh, S. Ryu, J. W. Palmour, A. R. Hefner, and J.-S. Lai, "1500 V, 4 A 4H-SiC JBS Diodes," *Proceedings of IEEE International Symposum on Power Semiconductor Devices and ICs (ISPSD)*, May 2000.

[4] R. W. Erickson, *Fundamentals of Power Electronics*, Chapman & Hall, New York, NY, 1997.

[5] L. Lorenz, M. Marz, and G. Deboy, "An Important Milestone Towards a New Power MOSFET Generation," *Proceedings of PCIM Power Conversion*, May 1998, pp. 151–160.

[6] J.-S. Lai, B. M. Song, R. Zhou, A. R. Hefner., D. W. Berning, and C.-C. Shen, "Characteristics and Utilization of a New Class of Low On-Resistance MOS-Gated Power Device," *Conf. Rec. of IEEE IAS Annual Meeting*, Oct. 1999, pp. 1073-1079.

[7] H. Zhu, Y. Tang, J.-S. Lai, A. R. Hefner, "Analysis of Conducted EMI Emissions from PWM Inverter Based on Empirical Models and Comparative Experiments," *Conf. Rec. of IEEE Power Electronics Specialists Conf (PESC)*, 1999, pp. 1727-1733.